ADVANCES IN ATMOSPHERIC SCIENCES, VOL. 34, OCTOBER 2017, 1249–1262

• **Original Paper** •

Evolution of Surface Sensible Heat over the Tibetan Plateau Under the Recent Global Warming Hiatus

Lihua ZHU[1,2,3], Gang HUANG*[1,2,4,5], Guangzhou FAN[3,6], Xia QU[7], Guijie ZHAO[1,2], and Wei HUA[3]

[1]*State Key Laboratory of Numerical Modeling for Atmospheric Sciences and Geophysical Fluid Dynamics, Institute of Atmospheric Physics, Chinese Academy of Sciences, Beijing* 100029*, China*

[2]*University of Chinese Academy of Sciences, Beijing* 100049*, China*

[3]*School of Atmospheric Sciences/Plateau Atmosphere and Environment Key Laboratory of Sichuan Province/Joint Laboratory of Climate and Environment Change, Chengdu University of Information Technology, Chengdu* 610225*, China*

[4]*Laboratory for Regional Oceanography and Numerical Modeling, Qingdao National Laboratory for Marine Science and Technology, Qingdao* 266237*, China*

[5]*Joint Center for Global Change Studies, Beijing* 100875*, China*

[6]*Collaborative Innovation Center on Forecast and Evaluation of Meteorological Disasters, Nanjing University of Information Science and Technology, Nanjing* 210044*, China*

[7]*Center for Monsoon System Research, Institute of Atmospheric Physics, Chinese Academy of Sciences, Beijing* 100029*, China*

(Received 4 December 2016; revised 10 May 2017; accepted 18 May 2017)

ABSTRACT

Based on regular surface meteorological observations and NCEP/DOE reanalysis data, this study investigates the evolution of surface sensible heat (SH) over the central and eastern Tibetan Plateau (CE-TP) under the recent global warming hiatus. The results reveal that the SH over the CE-TP presents a recovery since the slowdown of the global warming. The restored surface wind speed together with increased difference in ground-air temperature contribute to the recovery in SH. During the global warming hiatus, the persistent weakening wind speed is alleviated due to the variation of the meridional temperature gradient. Meanwhile, the ground surface temperature and the difference in ground-air temperature show a significant increasing trend in that period caused by the increased total cloud amount, especially at night. At nighttime, the increased total cloud cover reduces the surface effective radiation via a strengthening of atmospheric counter radiation and subsequently brings about a clear upward trend in ground surface temperature and the difference in ground-air temperature. Cloud–radiation feedback plays a significant role in the evolution of the surface temperature and even SH during the global warming hiatus. Consequently, besides the surface wind speed, the difference in ground-air temperature becomes another significant factor for the variation in SH since the slowdown of global warming, particularly at night.

Key words: surface sensible heat, Tibetan Plateau, ground-air temperature difference, surface wind speed, global warming hiatus

Citation: Zhu, L. H., G. Huang, G. Z. Fan, X. Qu, G. J. Zhao, and W. Hua, 2017: Evolution of surface sensible heat over the Tibetan Plateau under the recent global warming hiatus. *Adv. Atmos. Sci.*, **34**(10), 1249–1262, doi: 10.1007/s00376-017-6298-9.

1. Introduction

The Tibetan Plateau (TP) is renowned worldwide for its high elevation, vast area and highly complex terrain. It is a huge heat source towering in the free atmosphere, transferring heat from the land surface to the air in the form of sensible heating, latent heat transfer, and effective radiation of the ground (Yeh et al., 1957; Yeh and Gao, 1979). With its thermal forcing and dynamic forcing, the TP dominates the climate pattern of the Eurasian continent and, moreover, it affects changes in atmospheric circulation and the formation of climate in China, Asia, and even the whole world (Yeh et al., 1957; Yeh and Gao, 1979; Yanai et al., 1992; Ye and Wu, 1998; Duan and Wu, 2005; Duan et al., 2012; Wu et al., 2012). Hence, the TP is an important area of study in the field of meteorology.

Duzheng YE is widely regarded as the founder of the field of TP meteorology. In the late 1950s, Yeh et al. (1957) demonstrated for the first time that the TP is a heat source

* Corresponding author: Gang HUANG
Email: hg@mail.iap.ac.cn

for the atmosphere in summer. From then on, through analyses using different calculation methods and various data, the spatiotemporal characteristics of the heating field over the TP and their effect upon weather and climate have become an important avenue of research in meteorology (Yeh et al., 1958; Yeh and Gao, 1979; Wu et al., 1997, 2004, 2012; Duan and Wu, 2005, 2008; Yang et al., 2011a, 2011b; Duan et al., 2013; Chen et al., 2015; Hu and Duan, 2015).

Studies in recent years have pointed out that the surface sensible heat (SH), one component of the heat source over the TP, exhibits a remarkable decreasing trend since the mid-1980s, induced primarily by weakened surface wind speed (Duan and Wu, 2008). Furthermore, the trend in surface wind and the associated SH over the TP is related to the decreased East Asian subtropical westerly jet (EASWJ), which is mainly a response to the spatially inhomogeneous large-scale warming over the East Asian continent, marked by a much larger warming amplitude in middle and high latitudes than that over the tropics and subtropics region. That gives rise to a decreasing tendency in meridional pressure gradient and, accordingly, a decreased EASWJ (Duan and Wu, 2009; Duan et al., 2011). In other words, the weakening trend in surface SH flux is a consequence of regional nonuniformity in global warming. However, global mean surface and tropospheric temperatures have presented a warming slowdown since the late 1990s (Meehl et al., 2011; Kosaka and Xie, 2013; England et al., 2014; Santer et al., 2014; Schmidt et al., 2014; Dai et al., 2015; Trenberth, 2015). How, then, does the spatial distribution of the trend in air temperature change over the East Asian continent during this global warming hiatus? Does the meridional pressure gradient related to the EASWJ alter during that period? If there are any changes, what are they and how does the surface wind speed associated with the SH over the TP change? And is the surface wind speed still the dominant factor affecting SH over the TP during the ongoing warming hiatus? This paper seeks to answer these questions one by one.

The overall structure is as follows: Section 2 briefly describes the data and methodology applied in the study. The variation in SH is discussed in section 3. The reason for the recovery in SH under the global warming hiatus is investigated in section 4, followed by a summary and discussion in section 5.

2. Data and methodology

2.1. *Data*

The data used in this study include the following sources:

(1) The regular surface meteorological observations for the TP area offered by the China Meteorological Administration (CMA). The details of the dataset parallel those of Duan and Wu (2008), except that the data period in this study is from January 1980 to December 2015.

(2) The monthly mean air temperature, geopotential height, zonal wind speed, and six-hourly mean of total cloud cover (TCC) and radiation flux at the surface (downward longwave radiation, downward solar radiation, upward longwave radiation, and upward solar radiation) from the National Centers for Environmental Prediction/Department of Energy (NCEP/DOE) reanalysis 2 are applied to analyze the variations in circulation. The data periods are all from January 1980 to December 2015 (https://www.esrl.noaa.gov/psd/data/gridded/data.ncep.reanalysis2.html).

The locations and elevations of the stations are shown in Fig. 1, most of which are located in Qinghai, Xizang, and the western plateau of Sichuan in China. The data cover the central and eastern TP (CE-TP) domain (25°–40°N, 85°–108°E) with 129 stations. However, there are only 12 stations over the western TP (W-TP), most of which are located at the northern edge of the plateau. Consequently, we mainly discuss the variation in local surface SH transfer over the CE-TP. In addition, the method of processing missing values in the data are the same as applied in Duan and Wu (2008). In

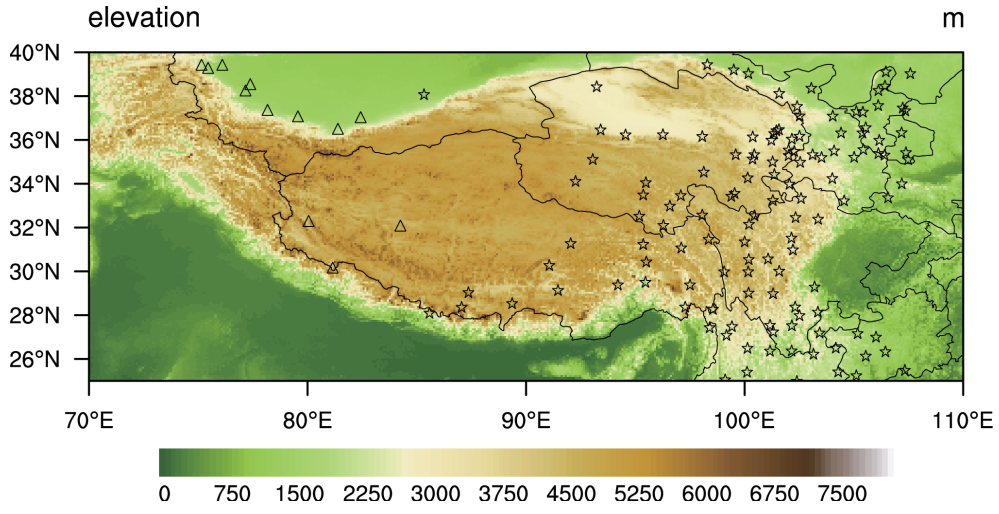

Fig. 1. Locations of stations at or higher than 1000 m and their elevations. Triangles and stars denote stations over the W-TP and CE-TP, respectively.

general, the missing values of variables account for less than 0.5% of the total records.

2.2. *Methods*

The methods for calculating the SH are the same as employed in previous studies (e.g., Yeh and Gao, 1979; Chen et al., 1985; Li et al., 2001; Duan and Wu, 2008; Duan et al., 2011):

$$\mathrm{SH} = C_p \rho_a C_{\mathrm{DH}} V_0 (T_s - T_a) \,. \tag{1}$$

Descriptions of the physical quantities in the above formula are available in the referenced literature. What is different, however, is that the present study takes the air density as a variable, considering the large elevation span. The air density is calculated as

$$\rho_a = 1.293 \left(\frac{P}{P_0}\right)\left(\frac{273.15}{T_a}\right) , \tag{2}$$

where P is surface pressure, P_0 is standard atmospheric pressure, and T_a is surface air temperature. In this study, $C_p = 1005$ J kg^{-1} K^{-1} is the specific heat of dry air at constant pressure, and we assume $C_{\mathrm{DH}} = 4 \times 10^{-3}$ (Li and Yanai, 1996; Duan and Wu, 2008) for the CE-TP. In this way, the surface wind speed (V_0), the difference in ground-air temperature ($T_s - T_a$) and the air density (ρ_a) are the three key factors influencing the evolution of SH. To identify which is the main impact factor among these three, the correlation degree method (Wei, 1999) is applied to calculate the optimal sequence in terms of their influence on the trend in SH.

3. Evolution of SH over the CE-TP

3.1. *Evolution of SH during day and night*

According to previous studies, SH reaches its daily minimum during the night and maximum at noon (Duan and Wu, 2008). Hence, the temporal evolution of T_s, T_a, $T_s - T_a$, ρ_a, V_0 and SH, averaged over the CE-TP at 0000 and 1200 local standard time (LST) for the period 1980–2015, is displayed in Fig. 2 to estimate their linear variation trend (LVT), to determine the main factor, and to find out their differences between day and night.

At night (0000 LST), T_s and T_a have similar interannual variations and decadal trends, which all represent an increasing tendency during 1980–2015, with LVTs of 0.54°C (10 yr)$^{-1}$ (exceeding the 99% confidence level) and 0.36°C (10 yr)$^{-1}$ (at the 99% confidence level), respectively. In particular, a larger increase in T_s than in T_a since the end of the 20th century leads to an increase in $T_s - T_a$ thereafter. Meanwhile, the ρ_a decreases continuously from the 1980s, with an LVT of −0.0012 kg m^{-3} (10 yr)$^{-1}$, which is significant at the 99% confidence level. The non-persistent rise in V_0 after the early 2000s reverses its steady slump before that time. The combined effect of the changes in $T_s - T_a$, ρ_a and V_0 lead to a slight increasing trend of SH before about 1998 and a significant increment thereafter, with trend coefficients of 1.87 W m^{-2} (10 yr)$^{-1}$ (at the 99% confidence level).

At 1200 LST, the trends in T_s [0.60°C (10 yr)$^{-1}$], T_a [0.54°C (10 yr)$^{-1}$] and ρ_a [0.0018 kg m^{-3} (10 yr)$^{-1}$] are similar to those at 0000 LST, except that they have small changes in amplitude. Compared with the variation at night, the $T_s - T_a$ during daytime presents a slight increasing trend, followed by a decreasing tendency, during the last dozen years. In addition, the V_0 at noon shows a remarkably weakening trend of −0.23 m s^{-1} (10 yr)$^{-1}$ before 1998 (exceeding the 99% confidence level), followed by changes with no obvious tendency. The changes in the above factors together induce the significant decreases in SH at 1200 LST, with a trend of −10.5 W m^{-2} (10 yr)$^{-1}$ (at the 99% confidence level), in the period between 1980 and 1997, before a stagnation in the weakening trend from around 1998.

According to the above analysis, the evolution of SH is similar to that of $T_s - T_a$ at night, while it has a resemblance with the variation in V_0 and ρ_a at noon. But is the ground-air temperature difference ($T_s - T_a$) the main impact factor in the variation of SH at night? And which factor is the major contributor to the trend in SH during daytime: the wind speed (V_0) or the air density (ρ_a)? To quantitatively analyze these aspects, the correlation degree method is applied to identify the optimal sequence of the three factors' ($T_s - T_a$, V_0, and ρ_a) influences on SH. The correlation degree between SH and the three factors is shown in Table 1. It is clear that, at 0000 LST, the trend in SH is most closely related with the change in $T_s - T_a$. The correlation degree is 0.999, followed by V_0 (correlation degree of 0.711), and then ρ_a (correlation degree of 0.558). Meanwhile, at 1200 LST, the optimal sequence regarding the three factors' impacts on the trend in SH is as follows: V_0, ρ_a and $T_s - T_a$, with correlation degrees of 0.998, 0.852 and 0.792, respectively.

3.2. *Seasonal evolution of SH*

The temporal evolutions of T_s, T_a, $T_s - T_a$, ρ_a, V_0 and SH during the four seasons are exhibited in Fig. 3. The T_s and T_a have similar interannual variations and decadal increasing trends in the four seasons during 1980–2015. Also, it is noteworthy that, since the turn of the 20th century, the $T_s - T_a$ in the four seasons presents an abrupt climatic change, which is just like the evolution of $T_s - T_a$ at night shown in Fig. 2. This implies that most contributions to the daily mean $T_s - T_a$ come from its evolution at night during that period. The air density (ρ_a) over the CE-TP shows a steady downward trend year-round, except for some differences in the extent of decline. At the end of the 20th century, the persistent decline in the winds in all seasons is reversed and replaced by a smooth change or slight rise.

Table 1. Correlation degree between SH and various factors at 0000 LST and 1200 LST.

	Correlation degree	
	0000 LST	1200 LST
$T_s - T_a$	0.999	0.792
V_0	0.711	0.998
ρ_a	0.558	0.852

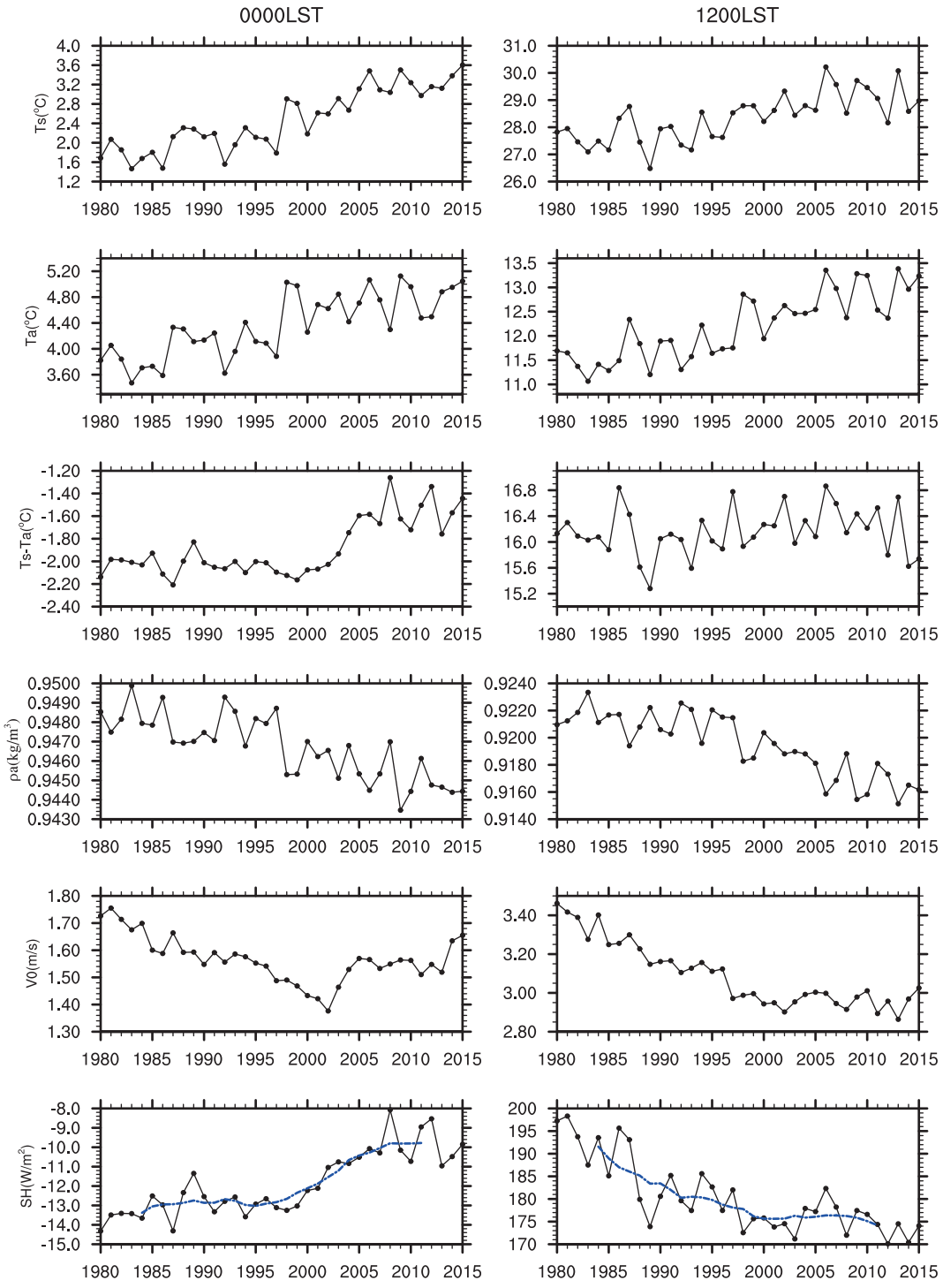

Fig. 2. Temporal evolution of 129-station-averaged T_s, T_a, $T_s - T_a$, ρ_a, V_0 and SH over the CE-TP during 1980–2015, at 0000 LST (left-hand panels) and 1200 LST (right-hand panels). The lines in blue indicate the nine-year moving average of SH.

The combined effect of the changes in $T_s - T_a$, V_0 and ρ_a leads to a decreasing trend in SH before the 21st century, especially in winter and spring, which is mainly composed of the variations in SH during daytime (as shown in Fig. 2). Accordingly, compared with $T_s - T_a$, V_0 or ρ_a may contribute more to the trend in SH during that period, in particular in winter and spring; while after that time, a weak increment in SH emerges that basically reflects the combined nighttime and daytime trend. It is possible that the former factor is more important than the latter (see Fig. 2), which may explain why the trends in SH in the four seasons since the end of the 20th century seem most closely related with the changes in $T_s - T_a$, followed by V_0 and ρ_a.

One notable aspect is that the transition period of the

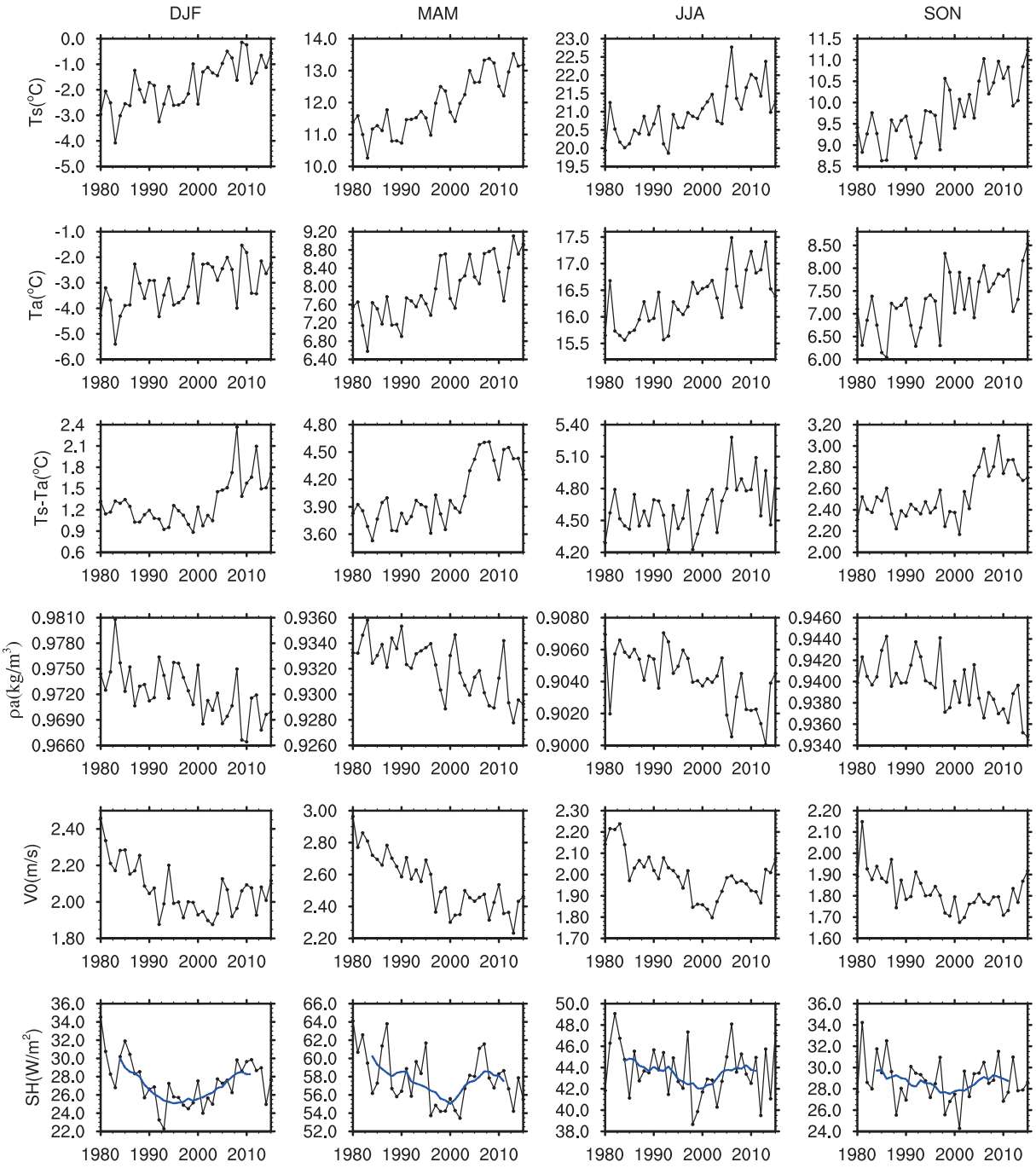

Fig. 3. Temporal evolution of 129-station-averaged T_s, T_a, $T_s - T_a$, ρ_a, V_0 and SH over the CE-TP during 1980–2015, for December–February (DJF; left-hand column), MAM and JJA (middle two columns), and September–November (SON; right-hand column). The lines in blue indicate 9-year moving average of SH.

trends in SH and its associated factors over the CE-TP corresponds closely to the period when a marked hiatus occurs in global surface warming, as reported in many studies (e.g., Meehl et al., 2011; Kosaka and Xie, 2013; England et al., 2014; Santer et al., 2014; Schmidt et al., 2014; Dai et al., 2015; Trenberth, 2015). Therefore, here, the correlation degree between SH and various factors, in all seasons before and after 1998, which is considered as the beginning of the global warming hiatus (Santer et al., 2011, 2013; Solomon et al., 2011; Fyfe et al., 2013a, 2013b), is used to carry out a quantitative evaluation to substantiate the conjecture above.

We can identify from Table 2 that, compared with the other two factors, surface wind speed (V_0) is the main impact factor for SH in winter and spring during the period 1980–97, while the SH in summer and autumn is influenced mainly by $T_s - T_a$ in this period (although, the effect of wind speed during that period cannot be neglected). In contrast, the effect of the evolution of $T_s - T_a$ on SH after 1998 becomes even more significant than that before, as well as more remarkable than the influence of V_0 over the same period in all seasons.

Table 2. Correlation degree between SH and various factors ($T_s - T_a$, V_0 and ρ_a) in all seasons.

	Correlation degree							
	DJF	MAM	JJA	SON	DJF	MAM	JJA	SON
	(1980–1997)				(1998–2015)			
$T_s - T_a$	0.894	0.941	0.973	0.988	0.987	0.950	0.997	0.992
V_0	0.999	0.977	0.959	0.984	0.871	0.920	0.950	0.927
ρ_a	0.690	0.804	0.738	0.775	0.770	0.847	0.702	0.831

The impact of wind speed on SH diminishes somewhat during 1998–2015 compared with 1980–97. Besides, the air density is always the least important factor of the three, yearround, during 1980–97 and 1998–2015. This indicates that the impact of the evolution of $T_s - T_a$ on SH becomes increasingly dominant in all seasons during the global warming hiatus. Furthermore, the effect of the change in $T_s - T_a$ on the evolution of SH mainly occurs at night, according to Fig. 2 and Table 1.

To sum up, firstly, the decreasing surface wind speed (V_0) is the main impact factor for SH during the period 1980–97 (Fig. 3, Table 2); and secondly, the effect of $T_s - T_a$ on SH becomes increasingly significant after 1998. Furthermore, the increasing $T_s - T_a$, especially at night, reverses the decreasing trend in SH before around 1998, which is clearly presented in Figs. 2 and 3 and Tables 1 and 2.

4. Reason for the recovery in SH under the global warming hiatus

The next consideration is whether the evolution of the surface SH transfer over the TP has a connection with the recent global warming hiatus. Based on previous research (Duan and Wu, 2008, 2009; Duan et al., 2011), the decreasing trend in SH over the TP since the 1980s is related to the decreased EASWJ, which is due to the spatial nonuniformity of global warming over the East Asian continent. However, since the end of the 20th century, the observed global-mean surface temperature displays little increase, or even a slight negative trend (Easterling and Wehner, 2009), which may lead to the changes in the spatial distribution of the trend in air temperature over the East Asian continent. The spatial inhomogeneity of surface global warming or cooling may distinctly alter the surface wind speed at a regional scale via atmospheric thermal adaption (Lin et al., 2013). Furthermore, the remarkable variety in surface wind speed corresponds to changes in upper-air zonal wind and the pressure gradient (Zhang et al., 2009). In this way, the recovery of wind speed since the beginning of the 2000s over the TP might be ascribed to the warming gradient and atmospheric circulation adjustment (Lin et al., 2013).

Additionally, a striking warming over the TP during recent decades has been revealed by many studies (e.g., Duan et al., 2006; Liu et al., 2009). Furthermore, compared with 1980–97, an accelerated warming trend is apparent over the TP during 1998-2013 (Duan and Xiao, 2015). More importantly, the climate warming over the TP is characterized by a significant increase in the nocturnal surface air temperature (Duan et al., 2006). And to some extent, the warming during the 20th century is caused by the daily minimum temperature increasing at a faster rate than the daily maximum (Karl et al., 1991, 1993; Easterling et al., 1997). Thus, the imbalanced rate of temperature change leads to a decreasing trend in the diurnal temperature range in most areas. The variety in cloud amount contributes to at least part of the warming in surface air temperature and its decreasing diurnal range over the TP (Duan et al., 2006). So, the changes in cloud amount may also lead to the variations in $T_s - T_a$ over the CE-TP, especially at night, during the global warming hiatus.

According to the results presented in section 3, V_0 and $T_s - T_a$ are the dominant factors involved in the evolution of SH during the global warming hiatus. Consequently, we next discuss the causes of the evolution of these two factors to explore the reason for the recovery in SH under the global warming hiatus.

4.1. *Reason for the recovery in V_0 under the global warming hiatus*

Relatively high values of SH over the CE-TP appear in spring and summer; consequently, the LVTs for air temperature, geopotential height, and zonal wind speed at 500 hPa in spring and summer are discussed to assess the relationship between the evolution of V_0 and the global warming hiatus.

Figure 4 shows the spatial distribution of LVTs for air temperature and geopotential height at 500 hPa in spring and summer during 1980–97 and 1998–2015. In spring, a warming trend of 0.2°C (10 yr)$^{-1}$–0.6°C (10 yr)$^{-1}$ is found over Baikal and Mongolia, while a much weaker warming trend, or even cooling trend, exists over subtropical Asia during 1980–97 (Fig. 4a). This characteristic of a larger warming over the midlatitudes than over the tropics and subtropics is more obvious in summer of that period. A substantial warming trend, with a central value of more than 0.4°C (10 yr)$^{-1}$, spreads over the whole of Mongolia; meanwhile, a cooling trend sweeps across the tropics and subtropics of East Asia in summer (Fig. 4e). All these factors cause the rise in geopotential height over the middle and high latitude areas in the north of the CE-TP and the fall in the tropics and subtropics to the south of the TP (Figs. 4c and g). Ultimately, that could lead to a further dwindling of the meridional pressure gradient and, thereafter, a diminishing zonal wind speed located to the south of the warming center. This confirms the results in Zhang et al. (2009).

Compared with the period 1980–97, a less obvious warming signal, or even cooling trend, is found to the north of the CE-TP from spring to summer during 1998–2015. Moreover, in subtropical Asia, there is an increasing trend or weak decreasing signal (Figs. 4b and f). Thus, geopotential height drops in cooling areas but rises in warming regions (Figs. 4d and h), which is due to the changes in temperature. Thus, the continuously diminishing meridional pressure gradient in the earlier stage can be alleviated during the global warming

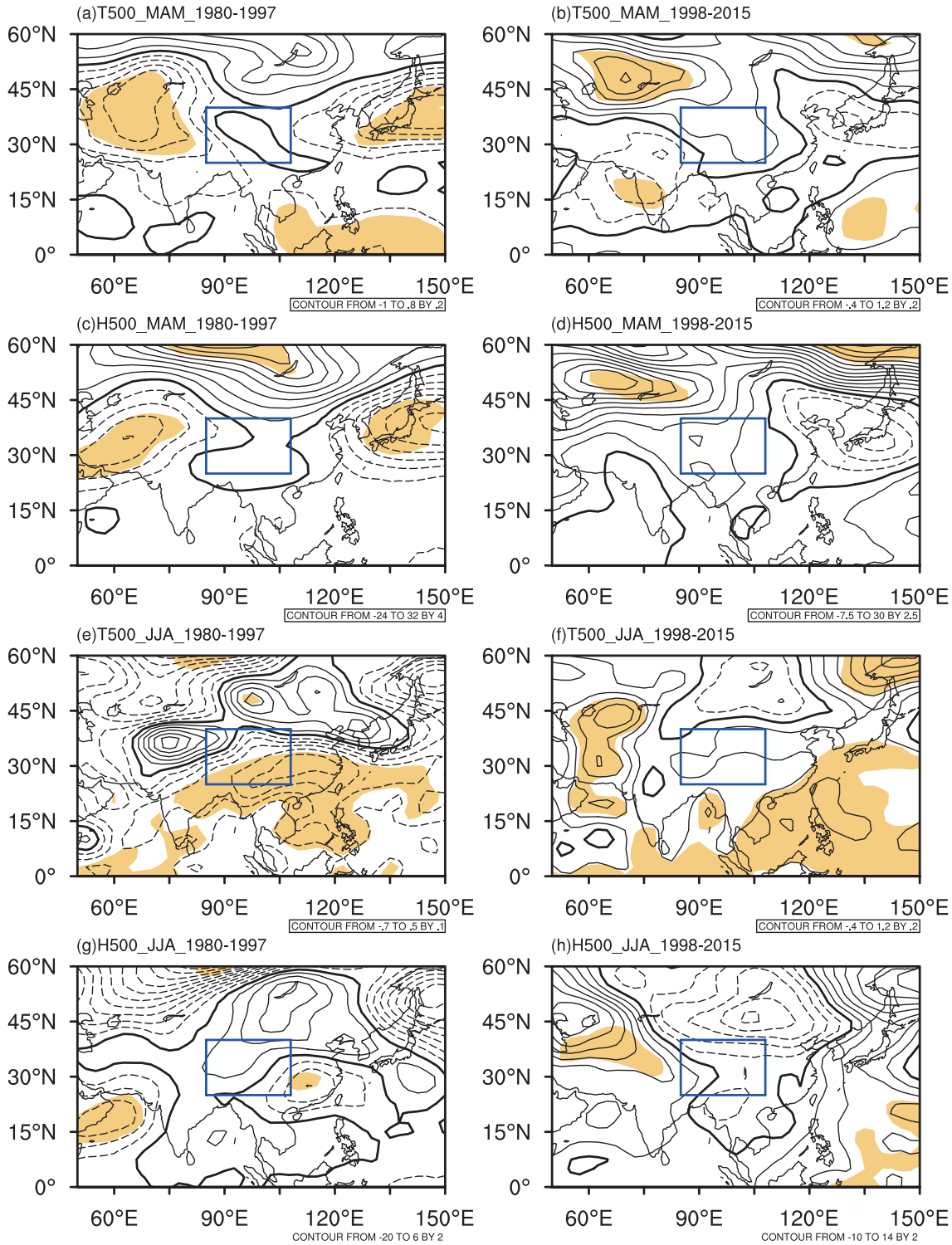

Fig. 4. Spatial distribution of LVTs for (a, b, e, f) air temperature [°C (10 yr)$^{-1}$] and (c, d, g, h) geopotential height [m (10 yr)$^{-1}$] at 500 hPa, in spring (MAM) and summer (JJA), during 1980–1997 (left-hand panels) and 1998–2015 (right-hand panels). The blue rectangle denotes the CE-TP area. Shaded areas denote a significant trend at the 90% level.

slowdown and, subsequently, the persistent weakening is substituted by a slight decrease or even a slender positive trend in zonal wind, as well as surface wind speed, over the CE-TP, whose mean altitude is about 600 hPa and the surface airflow is dominated primarily by the EASWJ in the mid-troposphere. This agrees with the conclusions in Lin et al. (2013).

To further illustrate the evolution of the zonal wind over the East Asian subtropical region during the two periods (1980–97 and 1998–2015), we investigate the change in the

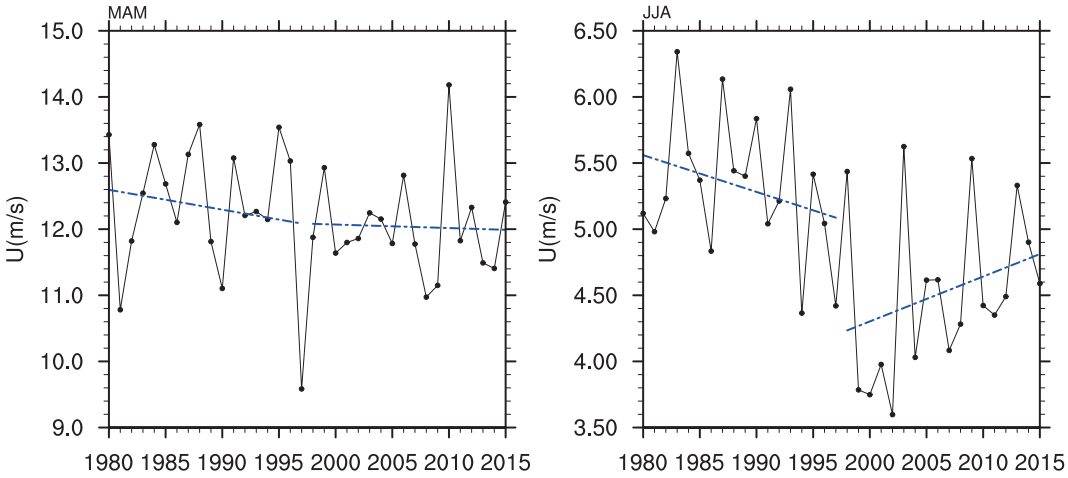

Fig. 5. Temporal evolution (solid curves in black) and LVTs (dashed lines in blue) of the 500-hPa zonal wind in spring and summer averaged over (25°–45°N, 80°–120°E). Units: m s^{-1}.

zonal wind speed at 500 hPa in spring and summer averaged over (25°–45°N, 80°–120°E), and the temporal evolution and LVTs are shown in Fig. 5. A decreasing trend in midtropospheric zonal wind over the East Asian subtropical region is evident in March–April–May (MAM; −0.30 m s^{-1} (10 yr)$^{-1}$ and June–July–August (JJA; −0.28 m s^{-1} (10 yr)$^{-1}$ during 1980–97. Thereafter, an increasing trend replaces the declining tendency in spring and summer, with LVTs of −0.053 m s^{-1} (10 yr)$^{-1}$ and 0.34 m s^{-1} (10 yr)$^{-1}$, respectively. It is remarkable that the diminishing trend in zonal wind at 500 hPa before 1997, and the increasing tendency during the global warming hiatus, over the East Asian subtropical area, are both more obvious in summer compared to spring, which is due to the differences between spring and summer in the LVTs for air temperature and geopotential height, as shown in Fig. 4.

4.2. *Evolution in surface temperature during the global warming hiatus*

The T_s and T_a both show a continuous upward trend in MAM and JJA during 1980–97 and 1998–2015, except for the extent, as shown in Table 3. But, perhaps more significantly, against the background of the global warming hiatus, the T_s and T_a over the CE-TP still present a rapid, or even more prominent, warming during 1998–2015 compared with 1980–97. This is consistent with Duan and Xiao (2015). The LVTs for T_s in spring and summer during 1998–2015 are 0.75°C (10 yr)$^{-1}$ (at the 99% confidence level) and 0.44°C (10 yr)$^{-1}$ (at the 90% confidence level), respectively. These values are larger than in the period 1980–97, during which the LVTs are 0.28°C (10 yr)$^{-1}$ in spring and 0.19°C (10 yr)$^{-1}$ in summer. For 1998–2015, the LVT of T_a [0.32°C (10 yr)$^{-1}$] is larger than that in 1980–97 [0.23°C (10 yr)$^{-1}$] in spring. Similar to the case in MAM, in summer, the T_a in 1998–2015 [0.21°C (10 yr)$^{-1}$] shows a greater increasing tendency than in 1980–97 [0.15°C (10 yr)$^{-1}$]. The larger increase in T_s than in T_a since 1998 leads to a rise in $T_s - T_a$ in both seasons, with LVTs of 0.42°C (10 yr)$^{-1}$ (exceeding the 99% confidence level) and 0.23°C (10 yr)$^{-1}$ (at the 95% confidence level). Thus, the temporal evolutions of the $T_s - T_a$ in spring and summer both exhibit a significant increasing tendency during the global warming hiatus, as shown in Fig. 3. Consequently, there is a striking difference in the mean $T_s - T_a$ during 1980–97 and 1998–2015. A sliding *t*-test is subsequently conducted, based on the time series of the $T_s - T_a$ in spring and summer, and the results show that the $T_s - T_a$ mean value in both seasons displays an abrupt climate change in 1998, which exceeds the 95% confidence level when the sub-sequence lengths are 11, 13 and 15.

Table 3. LVTs for T_s [°C (10 yr)$^{-1}$], T_a [°C (10 yr)$^{-1}$] and $T_s - T_a$ [°C (10 yr)$^{-1}$] over the CE-TP during the periods 1980–97 and 1998–2015. Significance at the 90%, 95% and 99% levels is indicated by one, two and three asterisks, respectively.

	LVTs			
	MAM	JJA	MAM	JJA
	(1980–1997)		(1998–2015)	
T_s	0.28	0.19	0.75***	0.44*
T_a	0.23	0.15	0.32	0.21
$T_s - T_a$	0.05	0.03	0.42***	0.23**

Next, we try to identify the factors responsible for the rapid warming and the marked increase in $T_s - T_a$ over the CE-TP during the global warming hiatus. This may be due to the high altitude, complex terrain, as well as the resulting particular climatic environment over the TP. The TP is the largest and highest plateau in the world, often referred to as the "roof of the world" or the "third pole of the Earth" (in addition to the polar regions, the TP is home to Earth's largest cryosphere). The snow/ice cover of the surface has declined under global warming, leading to changes in the surface absorption of solar radiation and the enhancement of warming at higher altitudes (Giorgi et al., 1997; Chen et al., 2003; Berthier and Toutin, 2008; Liu et al., 2009; Rangwala et al., 2013; You et al., 2016). The positive feedback of the snow/ice albedo may account for the surface warming over the TP dur-

ing the global hiatus period (You et al., 2016). Moreover, the cloud–radiation feedback also plays a significant role in modulating the recent accelerating warming tendency over the TP (Duan and Xiao, 2015). Hence, in this study, we discuss the temporal evolution of TCC and radiation to assess the evolution in surface temperature under the global warming slowdown.

First, however, we need to consider that, during daytime, an increase in cloud amount brings about a diminishment in solar shortwave radiation reaching Earth's surface (Yang et al., 2012), and an enhancement of atmospheric counter radiation. These combined effects of radiation influence the role played by cloud in surface temperature changes. At night, an increase in cloud cover is conducive to surface warming through strengthening the atmospheric counter radiation and reducing the surface effective radiation. These changes in surface radiation energy are believed to be one of the immediate causes in the variation of surface temperature. Consequently, in order to further substantiate the conjecture above, we begin by discussing the relationship between the TCC and radiation during the global warming hiatus. This radiation includes downward solar radiation flux (DSRF) and downward longwave radiation flux (DLRF). The correlation coefficients are shown in Table 4.

Table 4 shows that solar radiation is highly and negatively correlated with TCC in spring and summer, while a significant positive correlation exists between longwave radiation and TCC. The correlation coefficients in Table 4 all exceed the 99% confidence level. This indicates that TCC is a substantial controlling factor for solar radiation and longwave radiation in spring and summer. Here, we discuss the daytime and nighttime temporal evolution of TCC and its relationship with surface temperature (T_s, T_a and $T_s - T_a$) separately.

The temporal evolutions of TCC, DLRF and DSRF over the CE-TP in spring and summer during 1980–2015 are shown in Figs. 6 and 7, respectively; and the correlation between TCC and T_s, T_a and $T_s - T_a$ over the CE-TP in spring and summer during 1998–2015 is presented in Table 5.

During the global warming hiatus, the TCC over the CE-TP presents an increasing tendency in both spring and summer, day or night (Fig. 6). Compared to summer, the increasing trend in TCC in spring is more notable, with an LVT of 4.82% (10 yr)$^{-1}$ (exceeding the 99% confidence level) at night and 2.76% (10 yr)$^{-1}$ (exceeding the 95% confidence level) during daytime. Meanwhile, the LVT in summer is 1.16% (10 yr)$^{-1}$ (below the 90% confidence level) at night time and 1.26% (10 yr)$^{-1}$ (below the 90% confidence level) during the day.

Table 4. Correlation coefficients between TCC and radiation in spring and summer during 1998–2015. Significance at the 90%, 95% and 99% levels is indicated by one, two and three asterisks, respectively.

	Correlation coefficients	
	MAM	JJA
DSRF	−0.648***	−0.945***
DLRF	0.769***	0.737***

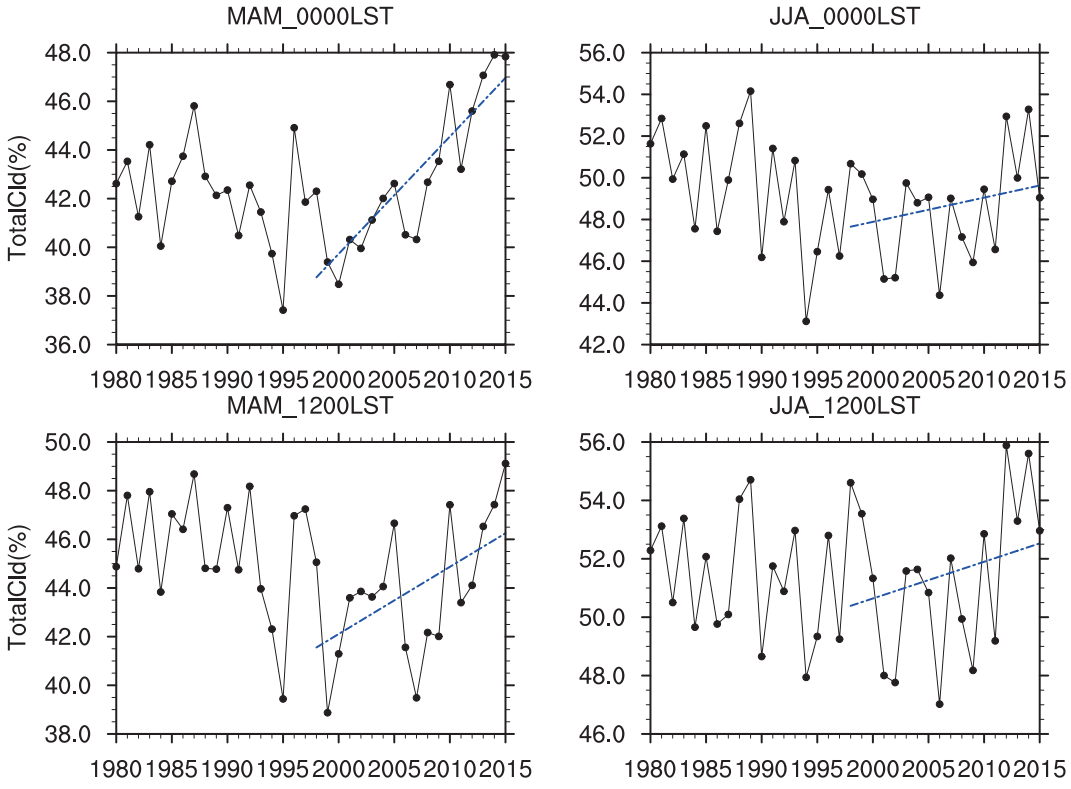

Fig. 6. Temporal evolution of TCC in the CE-TP in spring (MAM; left-hand panels) and summer (JJA; right-hand panels) during 1980–2015.

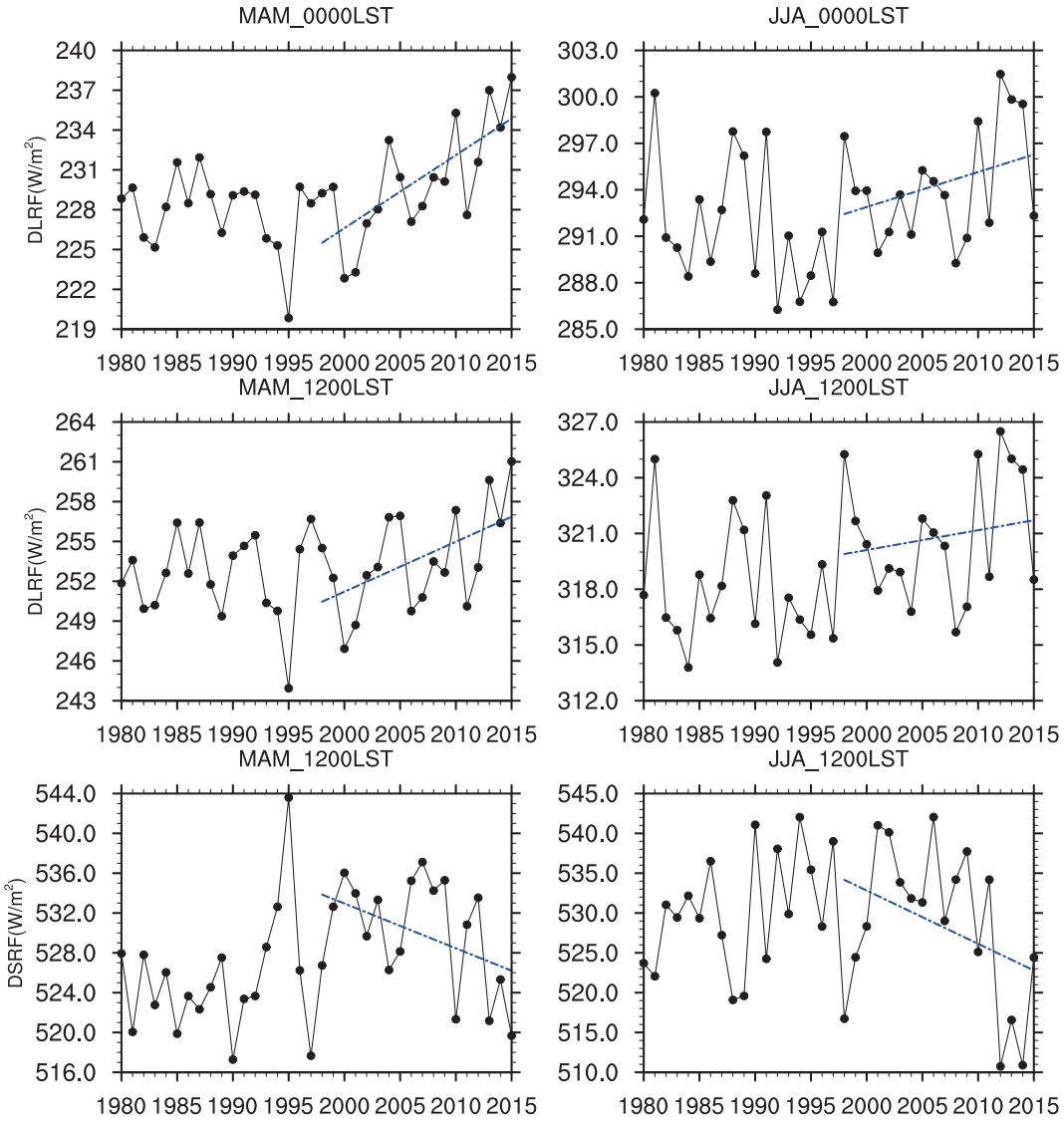

Fig. 7. Temporal evolution of DLRF and DSRF in the CE-TP in spring (MAM; left-hand panels) and summer (JJA; right-hand panels) during 1980–2015.

Table 5. Correlation coefficients between TCC and variables (T_s, T_a and $T_s - T_a$) in spring and summer during 1998–2015. Significance at the 90%, 95% and 99% levels is indicated by one, two and three asterisks, respectively.

	Correlation coefficients			
	MAM	JJA	MAM	JJA
	(0000 LST)		(1200 LST)	
T_s	0.589***	0.251	−0.027	−0.680***
T_a	0.407*	0.095	0.223	−0.303
$T_s - T_a$	0.540**	0.673***	−0.257	−0.813***

Thus, the increased TCC strengthens the DLRF through enhancing atmospheric counter radiation, both during the day and at night (Fig. 7). The LVT of the DLRF in spring is 5.5 W m^{-2} (10 yr)$^{-1}$ at night (99% confidence level) and 3.77 W m^{-2} (10 yr)$^{-1}$ during the daytime (95% confidence level). Meanwhile, the trends of DLRF in summer are less significant, with an LVT of 2.26 W m^{-2} (10 yr)$^{-1}$at night and 1.07 W m^{-2} (10 yr)$^{-1}$ during the daytime, which are both below the 90% confidence level. This is mainly due to the unapparent increase in TCC in summer (Fig. 6). Moreover, the DSRF dimming is primarily due to the diurnal increase in TCC. The LVT of DSRF in MAM and JJA is −4.5 W m^{-2} (10 yr)$^{-1}$ (90% confidence level) and −6.69 W m^{-2} (10 yr)$^{-1}$ (below the 90% confidence level), respectively (Fig. 7).

According to the analysis above, and Table 5, the correlation between the TCC and T_s and T_a over the CE-TP is positive at night and almost negative during the daytime. At night in spring, a significant positive correlation between the TCC and T_s exists over the CE-TP, with a correlation coefficient of 0.589 (99% confidence level), which is larger than that between TCC and T_a (0.407). Furthermore, an obvious positive correlation exists between TCC and $T_s - T_a$, with a correlation coefficient of 0.54, exceeding the 95% confidence

level. Compared with MAM, the relationships between TCC and T_s or T_a are both less significant in summer during the night, while the correlation with $T_s - T_a$ is remarkable (correlation coefficient of 0.673; 99% confidence level).

However, except for the T_a in MAM, negative correlation between TCC and T_s, T_a or $T_s - T_a$ occurs during the day in both seasons, owing to the greater effectiveness of the diminishment in solar shortwave radiation than in the enhancement of atmospheric counter radiation. Furthermore, they are both brought about by the increase in TCC. A significant negative correlation between TCC and T_s occurs in JJA, with a correlation coefficient of −0.68 (99% confidence level). Thus, the TCC in JJA has a prominent negative correlation with $T_s - T_a$ (correlation coefficient of −0.813; 99% confidence level).

To sum up, at night during the global warming hiatus, the increase in TCC brings about a strengthening of atmospheric counter radiation and a weakening of surface effective radiation, which subsequently causes an increase in downward net radiation flux at the surface (Fig. 8). Because of the smaller specific heat capacity on the ground compared with air the increased downward net radiation flux eventually results in a distinct increase in T_s and $T_s - T_a$.

The case during daytime is more complicated. The augmentation of TCC limits the amount of solar shortwave radiation reaching Earth's surface but, meanwhile, strengthens atmospheric counter radiation. The combined effect of TCC leads to variations in downward net radiation flux at the surface during the day, as shown in Fig. 8. During 1998–2015, the downward net radiation flux during the daytime in MAM and JJA presents a slight increasing trend, followed by a decreasing tendency. This brings about a less significant increment or declining trend in surface temperature during the daytime in that period. Consequently, the variation in $T_s - T_a$ is mainly affected by the changes in TCC at nighttime.

Consequently, cloud–radiation feedback plays a more significant role in the evolution of the $T_s - T_a$, and even the SH, during the global warming hiatus, particularly at night.

5. Summary and discussion

Using regular surface meteorological observations and NCEP/DOE reanalysis data, the evolution of surface SH over the CE-TP under the recent global warming hiatus is demonstrated in this study. The primary study outcomes are summarized as follows:

(1) At night, the SH over the CE-TP presents a slight increasing trend before 1998 and a significant increment during the global warming hiatus, which is mainly due to the variation in $T_s - T_a$. Meanwhile, during the daytime, the SH decreases significantly before 1998 and, subsequently, recovers in the period between 1998 and 2015; the wind speed is the major contributor to this variation.

(2) The SH shows a decreasing trend in all four seasons before 1998, especially in winter and spring, mainly manifested through the effect brought about by the weakening in V_0. This conclusion is consistent with the results in previous literature (Duan and Wu, 2008, 2009; Duan et al., 2011). But, more importantly, during the global warming hiatus, a weak

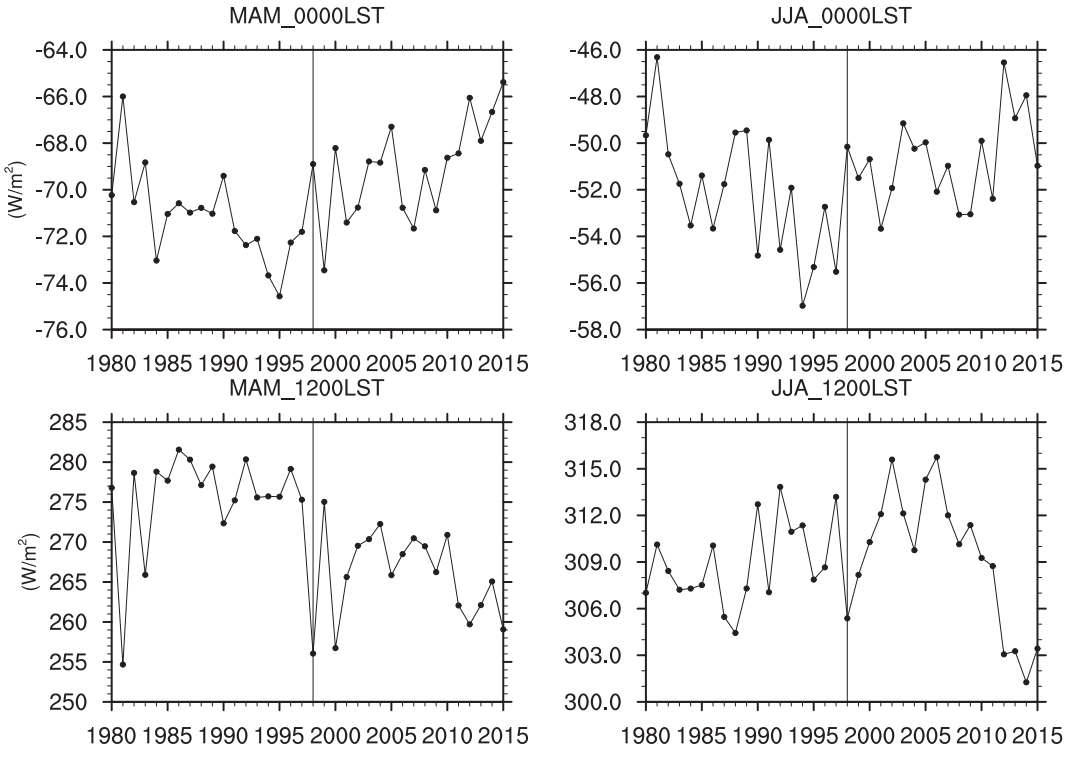

Fig. 8. Temporal evolution of downward net radiation flux at the surface in the CE-TP in spring (MAM; left-hand panels) and summer (JJA; right-hand panels) during 1980–2015.

increment in SH emerges, and it is most closely related with the recovery in V_0 and the increase in nocturnal $T_s - T_a$.

(3) In this study, we confirm previous research findings that the diminishing surface wind speed is the main factor weakening the SH during global warming. Meanwhile, during the global warming hiatus, a less obvious warming signal, or even cooling trend, exists to the north of the CE-TP. Meanwhile, an increasing trend or weak decreasing signal is found in subtropical Asia. This alleviates the persistent weakening meridional pressure gradient before that time. Thereafter, the continuously diminishing trend is replaced by a slight decreasing or even a slender positive trend in zonal wind, as well as surface wind speed, over the CE-TP.

(4) During the global warming hiatus, the TCC presents an increasing trend during the daytime and at night. Thus, at night, the increase in TCC strengthens the atmospheric counter radiation and lessens the surface effective radiation. This causes an increase in downward net radiation flux at the surface and eventually results in an obvious increase in $T_s - T_a$, and even in SH. During daytime, the augmentation of TCC limits the amount of solar shortwave radiation reaching Earth's surface but, meanwhile, strengthens atmospheric counter radiation. The combined effect leads to the variation in downward net radiation flux at the surface in the daytime, which does not show a clear upward trend like that at night. Consequently, the recovery in SH during the global warming hiatus is mainly ascribed to the restored surface wind speed together with the increased nocturnal $T_s - T_a$.

Several issues remain unsolved. For instance, in this study, we assume the heat transfer coefficient is a constant value; but in fact, it is altered considerably by atmospheric stability (Guo et al., 2011; Yang et al., 2011b). Hence, this may lead to some uncertainties in climate change studies of surface heat flux over the TP. In addition, what causes the changes in TCC over the TP during the global warming hiatus? Moreover, the discussion in this study focuses on the SH over the CE-TP; but how does the SH over the W-TP change during the recent global warming hiatus? Now that the variation in surface SH is known to connect closely with the recent global warming hiatus, what other variables, such as latent heat, radiation flux of the air column, and even the total atmospheric heat source over the TP, might be involved? These topics require further investigation, in particular to understand the mechanism of changes in various variables over the TP against the background of the global warming hiatus. Further examination of these issues will be conducted in the future via numerical simulations.

Acknowledgements. This paper is dedicated to the great founder of TP meteorology, Duzheng YE. The authors thank the CMA for kindly providing the observational data. We also thank the two anonymous reviewers and editor for their useful comments. This work was supported by the National Natural Science Foundation of China (41425019, 41661144016, 91537214) and the Public Science and Technology Research Funds Projects of the Ocean (201505013).

REFERENCES

Berthier, E., and T. Toutin, 2008: SPOT5-HRS digital elevation models and the monitoring of glacier elevation changes in North-West Canada and South-East Alaska. *Remote Sensing of Environment*, **112**(5), 2443–2454, doi: 10.1016/j.rse.2007.11.004.

Chen, B., W. C. Chao, and X. Liu, 2003: Enhanced climatic warming in the Tibetan Plateau due to doubling CO_2: A model study. *Climate Dyn.*, **20**(4), 401–413, doi: 10.1007/s00382-002-0282-4.

Chen, J. H., X. Q. Wu, Y. Yin, and H. Xiao, 2015: Characteristics of heat sources and clouds over eastern China and the Tibetan Plateau in boreal summer. *J. Climate*, **28**, 7279–7296, doi: 10.1175/JCLI-D-14-00859.1.

Chen, L. X., E. R. Reiter, and Z. Q. Feng, 1985: The atmospheric heat source over the Tibetan Plateau: May–August 1979. *Mon. Wea. Rev.*, **113**, 1771–1790, doi: 10.1175/1520-0493(1985)113<1771:TAHSOT>2.0.CO;2.

Dai, A. G., J. C. Fyfe, S. P. Xie, and X. G. Dai, 2015: Decadal modulation of global surface temperature by internal climate variability. *Nature Climate Change*, **5**, 555–559, doi: 10.1038/nclimate2605.

Duan, A. M., and G. X. Wu, 2005: Role of the Tibetan Plateau thermal forcing in the summer climate patterns over subtropical Asia. *Climate Dyn.*, **24**, 793–807, doi: 10.1007/s00382-004-0488-8.

Duan, A. M., and G. X. Wu, 2006: Change of cloud amount and the climate warming on the Tibetan Plateau. *Geophys. Res. Lett.*, **33**(22), L22704, doi: 10.1029/2006GL027946.

Duan, A. M., and Z. X. Xiao, 2015: Does the climate warming hiatus exist over the Tibetan Plateau? *Scientific Reports*, **5**, 13711, doi: 10.1038/srep13711.

Duan, A. M., and G. X. Wu, 2008: Weakening trend in the atmospheric heat source over the Tibetan Plateau during recent decades. Part I: Observations. *J. Climate*, **21**, 3149–3164, doi: 10.1175/2007JCLI1912.1.

Duan, A. M., and G. X. Wu, 2009: Weakening trend in the atmospheric heat source over the Tibetan Plateau during recent decades. Part II: Connection with climate warming. *J. Climate*, **22**, 4197–4212, doi: 10.1175/2009JCLI2699.1.

Duan, A. M., G. X. Wu, Q. Zhang, and Y. M. Liu, 2006: New proofs of the recent climate warming over the Tibetan Plateau as a result of the increasing greenhouse gases emissions. *Chinese Science Bulletin*, **51**, 1396–1400, doi: 10.1007/s11434-006-1396-6.

Duan, A. M., F. Li, M. R. Wang, and G. X. Wu, 2011: Persistent weakening trend in the spring sensible heat source over the Tibetan Plateau and its impact on the Asian summer monsoon. *J. Climate*, **24**, 5671–5682, doi: 10.1175/JCLI-D-11-00052.1.

Duan, A. M., G. X. Wu, Y. M. Liu, Y. M. Ma, and P. Zhao, 2012: Weather and climate effects of the Tibetan Plateau. *Adv. Atmos. Sci.*, **29**(5), 978–992, doi: 10.1007/s00376-012-1220-y.

Duan, A. M., M. R. Wang, Y. H. Lei, and Y. F. Cui, 2013: Trends in Summer Rainfall over China Associated with the Tibetan Plateau Sensible Heat Source during 1980-2008. *J. Climate*, **26**, 261–275, doi: 10.1175/JCLI-D-11-00669.1.

Easterling, D. R., and M. F. Wehner, 2009: Is the climate warming or cooling? *Geophys. Res. Lett.*, **36**, L08706, doi: 10.1029/2009GL037810.

Easterling, D. R., and Coauthors, 1997: Maximum and minimum temperature trends for the globe. *Science*, **277**, 364–367, doi:

10.1126/science.277.5324.364.

England, M. H., and Coauthors, 2014: Recent intensification of wind-driven circulation in the Pacific and the ongoing warming hiatus. *Nature Climate Change*, **4**, 222–227, doi: 10.1038/nclimate2106.

Fyfe, J. C., K. von Salzen, J. N. S. Cole, N. P. Gillett, and J.-P. Vernier, 2013a: Surface response to stratospheric aerosol changes in a coupled atmosphere-ocean model. *Geophys. Res. Lett*., **40**, 584–588, doi: 10.1002/grl.50156.

Fyfe, J. C., N. P. Gillett, and F. W. Zwiers, 2013b: Overestimated global warming over the past 20 years. *Nature Climate Change*, **3**, 767–769, doi: 10.1038/nclimate1972.

Giorgi, F., J. W. Hurrell, M. R. Marinucci, and M. Beniston, 1997: Elevation dependency of the surface climate change signal: A model study. *J. Climate*, **10**(2), 288–296, doi: 10.1175/1520-0442(1997)010<0288:EDOTSC>2.0.CO;2.

Guo, X. F., K. Yang, and Y. Y. Chen, 2011: Weakening sensible heat source over the Tibetan Plateau revisited: effects of the land–atmosphere thermal coupling. *Theor. Appl. Climatol*., **104**(1–2), 1–12, doi: 10.1007/s00704-010-0328-1.

Hu, J., and A. M. Duan, 2015: Relative contributions of the Tibetan Plateau thermal forcing and the Indian Ocean Sea surface temperature basin mode to the interannual variability of the East Asian summer monsoon. *Climate Dyn*., **45**, 2697–2711, doi: 10.1007/s00382-015-2503-7.

Karl, T. R., G. Kukla, V. N. Razuvayev, M. J. Changery, R. G. Quayle, R. R. Heim Jr., D. R. Easterling, and C. B. Fu, 1991: Global warming: Evidence for asymmetric diurnal temperature change. *Geophys. Res. Lett*., **18**, 2253–2256, doi: 10.1029/91GL02900.

Karl, T. R., and Coauthors, 1993: A new perspective on recent global warming: Asymmetric trends of daily maximum and minimum temperature. *Bull. Amer. Meteor. Soc*., **74**, 1007–1023, doi: 10.1175/1520-0477(1993)074<1007:ANPORG>2.0.CO;2.

Kosaka, Y., and S. P. Xie, 2013: Recent global-warming hiatus tied to equatorial Pacific surface cooling. *Nature*, **501**, 403–407, doi: 10.1038/nature12534.

Li, C. F., and M. Yanai, 1996: The onset and interannual variability of the Asian summer monsoon in relation to land-sea thermal contrast. *J. Climate*, **9**, 358–375, doi: 10.1175/1520-0442(1996)009<0358:TOAIVO>2.0.CO;2.

Li, W. P., G. X. Wu, Y. M. Liu, and X. Liu, 2001: How the surface processes over the Tibetan Plateau affect the summertime Tibetan Anticyclone-numerical experiments. *Chinese Journal of Atmospheric Sciences*, **25**, 809–816, doi: 10.3878/j.issn.1006-9895.2001.06.08. (in Chinese with English abstract)

Lin, C. G., K. Yang, J. Qin, and R. Fu, 2013: Observed coherent trends of surface and upper-air wind speed over China since 1960. *J. Climate*, **26**(9), 2891–2903, doi: 10.1175/JCLI-D-12-00093.1.

Liu, X. D., Z. G. Cheng, L. B. Yan, and Z. Y. Yin, 2009: Elevation dependency of recent and future minimum surface air temperature trends in the Tibetan Plateau and its surroundings. *Global and Planetary Change*, **68**(3), 164–174, doi: 10.1016/j.gloplacha.2009.03.017.

Meehl, G. A., J. M. Arblaster, J. T. Fasullo, A. X. Hu, and K. E. Trenberth, 2011: Model-based evidence of deep-ocean heat uptake during surface-temperature hiatus periods. *Nature Climate Change*, **1**, 360–364, doi: 10.1038/nclimate1229.

Rangwala, I., E. Sinsky, and J. R. Miller, 2013: Amplified warming projections for high altitude regions of the northern hemisphere mid-latitudes from CMIP5 models. *Environmental Research Letters*, **8**, 024040, doi: 10.1088/1748-9326/8/2/024040.

Santer, B. D., and Coauthors, 2011: Separating signal and noise in atmospheric temperature changes: The importance of timescale. *J. Geophy. Res*., **116**, D22105, doi: 10.1029/2011JD016263.

Santer, B. D., and Coauthors, 2013: Identifying human influences on atmospheric temperature. *Proceedings of the National Academy of Sciences of the United States of America*, **110**, 26–33, doi: 10.1073/pnas.1210514109.

Santer, B. D., and Coauthors, 2014: Volcanic contribution to decadal changes in tropospheric temperature. *Nature Geoscience*, **7**, 185–189, doi: 10.1038/ngeo2098.

Schmidt, G. A., D. T. Shindell, and K. Tsigaridis, 2014: Reconciling warming trends. *Nature Geoscience*, **7**, 158–160, doi: 10.1038/ngeo2105.

Solomon, S., J. S. Daniel1, R. R. Neely III, J.-P. Vernier, E. G. Dutton, and L. W. Thomason, 2011: The persistently variable "background" stratospheric aerosol layer and global climate change. *Science*, **333**, 866–870, doi: 10.1126/science.1206027.

Trenberth, K. E., 2015: Has there been a hiatus? *Science*, **349**, 691–692, doi: 10.1126/science.aac9225.

Wei, F. Y., 1999: *Technology of Statistical Diagnosis and Prediction of Modern Climate*. China Meteorological Press, Beijing, 296 pp. (in Chinese)

Wu, G. X., W.P. Li, H. Guo, 1997: *Sensible heat driven air-pump over the Tibetan-Plateau and its impacts on the Asian Summer Monsoon*. In: Ye DZ (ed) Collections on the Memory of Zhao Jiuzhang.Science Press, Beijing, pp 116–126.(in Chinese)

Wu, G. X., Y. M. Liu, J. Y. Mao, X. Liu, and W. P. Li, 2004: Adaptation of the atmospheric circulation to thermal forcing over the Tibetan Plateau. *Observation, Theory and Modeling of Atmospheric Variability. Selected Papers of Nanjing Institute of Meteorology Alumni in Commemoration for Professor Jijia Zhang*, X. Zhu, X. F. Li, and S. T. Zhou, Eds., World Scientific, 92–114, doi: 10.1142/9789812791139_0004.

Wu, G. X., Y. M. Liu, B. He, Q. Bao, A. M. Duan, and F. F. Jin, 2012: Thermal controls on the Asian summer monsoon. *Scientific Reports*, **2**, 404, doi: 10.1038/srep00404.

Yanai, M., C. F. Li, and Z. S. Song, 1992: Seasonal heating of the Tibetan Plateau and its effects on the evolution of the Asian summer monsoon. *J. Meteor. Soc. Japan*, **70**, 319–351, doi: 10.2151/jmsj1965.70.1B_319.

Yang, K., X. F. Guo, He J., J. Qin, and T. Koike, 2011a: On the climatology and trend of the atmospheric heat source over the Tibetan Plateau: An experiments-supported revisit. *J. Climate*, **24**, 1525–1541, doi: 10.1175/2010JCLI3848.1.

Yang, K., X. F. Guo, and B. Y. Wu, 2011b: Recent trends in surface sensible heat flux on the Tibetan Plateau. *Science China Earth Sciences*, **54**, 19–28, doi: 10.1007/s11430-010-4036-6.

Yang, K., B. H. Ding, J. Qin, W. J. Tang, N. Lu, and C. G. Lin, 2012: Can aerosol loading explain the solar dimming over the Tibetan Plateau? *Geophys. Res. Lett*., **39**, L20710, doi: 10.1029/2012GL053733.

Ye, D. Z., and G. X. Wu, 1998: The role of the heat source of the Tibetan Plateau in the general circulation. *Meteor. Atmos. Phys*., **67**(1–4), 181–198, doi: 10.1007/BF01277509.

Yeh, T. C., and Y. X. Gao, 1979: *Qinghai-Xizang Plateau Meteorology*. Science Press, Beijing, 1–278. (in Chinese)

Yeh, T. C., S. W. Lo, and P. C. Chu, 1957: The wind structure and heat balance in the lower troposphere over Tibetan Plateau and its surrounding. *Acta Meteorologica Sinica*, **28**, 108–121, doi: 10.11676/qxxb1957.010. (in Chinese with English abstract)

Yeh, T. C., S. Y. Dao, and M. T. Li, 1958: The abrupt change of circulation over northern hemisphere during June and October. *Acta Meteorologica Sinica*, **29**, 249–263. (in Chinese with English abstract)

You, Q. L., J. Z. Min, and S. C. Kang, 2016: Rapid warming in the Tibetan Plateau from observations and CMIP5 models in recent decades. *International Journal of Climatology*, **36**, 2660–2670., doi: 10.1002/joc.4520.

Zhang, X. Q., Y. Ren, Z.-Y. Yin, Z. Y. Lin, and D. Zheng, 2009: Spatial and temporal variation patterns of reference evapotranspiration across the Qinghai-Tibetan Plateau during 1971–2004. *J. Geophys. Res*., **114**, D15105, doi: 10.1029/2009JD011753.